Fatigue Life of Double Angle Tension Members

J. MICHAEL STALLINGS, THOMAS E. COUSINS, and BRADLEY P. CHRISTOPHER

INTRODUCTION

Alabama Department of Transportation (ALDOT) bridge inspectors discovered failed (cracked) filler plate welds in numerous double angle tension and compression members of the floortrusses of twin tied arch bridges on Interstate 1-65 in late 1990. A typical double angle truss member with a cracked filler plate weld is illustrated in Figure 1(a). Figure 1(b) is a cross section through the double angle member looking down toward the filler plate. The ends of the filler plates are attached to the back to back legs of the double angles with square groove welds. The welds are approximately two inches long (full width of filler plate) and are ground flush with the outside ends of the filler plates. Inspection of the failed welds indicates that the weld penetration is typically 3⁄16-in. or less.

The double angles and filler plates are made of unpainted A588 Grade 50 weathering steel. The bridge has been open to traffic since 1981 and has developed a protective layer of rust. The normal weathering of the A588 steel caused rust to build up between the angle legs and filler plates. Built up corrosion products in restricted areas, called pack rust, can generate pressures of up to 10 ksi as discussed by Kulicki[1] et al. The floortruss verticals and diagonals are 8-in. by 6-in. angles with long legs back to back. By considering a pressure of 10 ksi (shown as p in Figure 2) over the 2-in. by 8-in. area between an angle and a filler plate, the force (T in Figure 2) on the weld at each end of the filler plate is 80 kips. The stress applied to the weld (throat area approximately 3⁄16-in. × 2 inches = .375 in.^{2}) at the end of a filler plate is approximately 200 ksi. This value is almost three times the weld capacity of 70 ksi. Thus, confined rust is considered to be the cause of the filler plate weld failures in the double angle members.

The weld crack (failure plane) created by the pack rust is parallel to the applied stress on the double angle, and none of these type cracks have propagated into the angles, and pose no immediate threat to the integrity of the trusses. However, the possibility of the filler plate weld cracks causing fatigue cracks perpendicular to the applied stress in the double angle tension members provided the motivation for the work discussed by Stallings[2] et al. and summarized here. One maintenance strategy considered by ALDOT prior to this project was to remove the filler plates and grind out the welds. However, this would be very expensive. For the tension members alone in the northbound and southbound spans, approximately 960 filler plates would have to be removed.

The purpose of the work reported here is to address whether it is necessary to remove the filler plates and grind out the welds. Field measurements of stresses in the tension members due to trucks of known weight and trucks in normal traffic are used to determine the traffic loading stresses and overall behavior of the floortrusses for use in fatigue analyses. The major questions addressed in this paper are: 1) What are the nominal extreme fiber stress ranges due to axial load plus

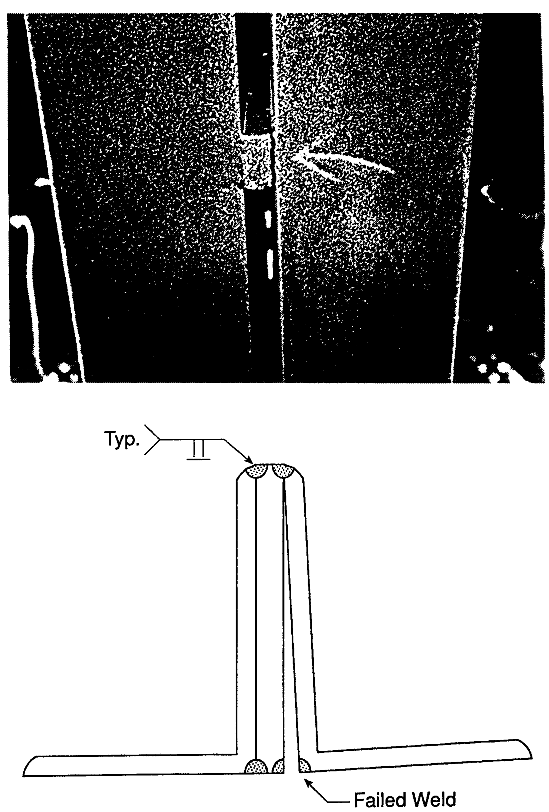

Fig. 1. Typical filler plate weld cracks in double angle truss members.

J. Michael Stallings is an associate professor, Department of Civil Engineering, Auburn University, Auburn, AL.

Thomas E. Cousins is an associate professor, Department of Civil Engineering, Auburn University, Auburn, AL.

Bradley P. Christopher is a design engineer with LaneBishop YorkDelahay Inc., Birmingham, AL, formerly a graduate student, Department of Civil Engineering, Auburn University.

bending near the filler plates in the floortruss tension members? 2) Are the extreme fiber stress ranges high enough to cause fatigue cracks to develop in the double angle members near the filler plate weld details? 3) If cracks initiate, will the cracks grow at a rate which would create a safety problem for traffic using the bridge?

BRIDGE DESCRIPTION AND TEST LOCATIONS

The twin steel tied arches span 800 ft. Fifteen interior floortrusses spaced at 50 ft. on center span 46 ft. transverse to the roadway between the arch tie girders. The vertical, diagonal, and bottom chord members of each floortruss consist of double angles that contain filler plates spaced at 2 ft. on center. The concrete deck slab is supported by six lines of stringers that run parallel to the direction of traffic, as shown in Figure 2. These lines are made of four units of stringers. Each unit is made continuous between expansion joints in the deck by splices placed at points where the bending moment is small. The stringers, which rest on top of each floortruss, are braced by diaphragms that run perpendicular to the traffic flow. Expansion joints in the deck system are located 200 feet apart at quarter points along the arch span (above the fourth, eighth, and twelfth floortrusses).

The primary field test locations along the arch span included floortrusses at quarter-span and mid-span. Each of these trusses were at expansion joint locations. To ensure that the presence of an expansion joint and brake in continuity in the floor system above a floortruss had little or no effect on the floortruss stresses, strain gages were installed along the neutral axis of two of the outer diagonal members of the floortruss located one panel away from the mid-span floortruss. As expected, the difference in stresses in the three floortrusses was minimal, and the major test locations chosen (quarter-span and mid-span) appear to be representative of all fifteen floortrusses of the arch span.

To differentiate between floortruss members an identification scheme is adopted here. This scheme is based on viewing the floortruss in the direction of traffic as shown in Figure 3. The six bottom chord members, starting from the right, were labeled B1 through B6. Similarly, the six diagonal members were labeled D1 through D6.

The exterior diagonals, D1 and D6, are double angles 8 × 6 × ¾-in. with long legs back to back. The interior diagonals D2 through D5, and the vertical members, are double angles 8 × 6 × ½-in. with long legs back to back. All bottom chord members are double angles 8 × 6 × ¾ with short legs back to back.

INSTRUMENTATION

Electrical resistance strain gages were used for measuring surface strains on the diagonal and bottom chord members. At the mid-span and quarter-span floortruss, 30 strain gages were installed, 16 on the bottom chord and 14 on the diagonal members. The strain gage locations are illustrated by the elevations and sections in Figures 4, 5 and 6. Only the diagonal members and bottom chord members are shown in Figures 4 and 6, respectively. The top chord, vertical members, and gusset plate details were omitted for clarity. Filler plates are indicated in the Figures by hidden lines.

The strain gage locations were chosen so that the live load stresses due to axial load and bending could be measured at critical cross sections adjacent to the filler plates in each member. Because the floortruss members are loaded only at the ends, the bending moments, and bending stresses, are largest at the filler plates nearest the member ends, and the axial stresses are constant along the length of the member. This means the combined tensile bending stress and axial stress is largest at the filler plates nearest the member ends. Hence, the filler plates nearest the ends of each member were

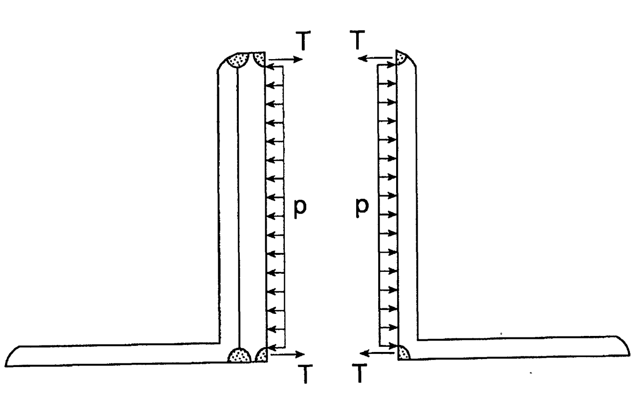

Fig. 2. Internal pressure and weld force from pack rust.

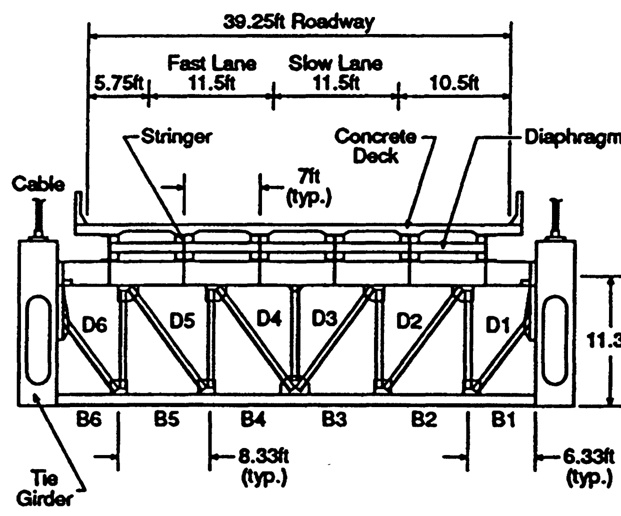

Fig. 3. Typical cross section through tied arch deck system.

considered to be the critical locations where fatigue cracking was most likely to occur.

Two strain gages were installed at one end of each member at a cross section adjacent to the edge of the filler plate nearest the end of the member as illustrated in Figure 5. The gages were placed 3 inches from the edge of the filler plate so that nominal stresses could be measured without the effects of the stress concentration due to the filler plates. The strain distribution across the member cross section was assumed to be linear, so the strain at the centroid (axial strain) and strains at the extreme fibers could be calculated from the two measured strains. A third gage was installed at the opposite end of selected members such as the upper end of diagonal D1 as shown in Figure 4. By using the strain measured at the centroid of the cross section at the lower end of member D1, and the single strain measurement at the upper end of the member, the extreme fiber strains could also be calculated at the upper end of the member.

The strain gage locations on the diagonal members were determined from a series of preliminary structural analyses of the floortruss using a general planar frame analysis computer program. The largest bending stresses were found at the upper end of the interior diagonals D2, D3, D4, and D5, so the strain gages were installed as shown in Figure 4. The critical stress locations on the outer diagonals were not as easily located because of uncertainty about the stiffness of the connection to the tie girder at the upper end of the member, so both ends of the exterior diagonal were instrumented.

DATA ACQUISITION

All field test data were collected with a data acquisition system capable of recording data from multiple channels at an overall rate of 25,000 samples per second. A recording rate of 400 samples per second per channel was used in making the dynamic strain measurements reported here. A maximum of thirty-two channels was utilized. Strain measurements for all gages at the quarter span floortruss were made simultaneously. Measurements for all gages at the midspan floortruss and at the floortruss one panel away were made simultaneously. A 486-33 MHz personal computer equipped with compatible software was used to drive the data acquisition system. All data were recorded and temporarily stored on the personal computer hard disk. The data were backed up onto magnetic tape at the end of each day.

To obtain unbiased stress measurements due to normal truck traffic, all computer and data acquisition equipment and supplies were kept beneath the bridge and out of sight of passing traffic. This was accomplished by using temporary work platforms supported on the horizontal wind bracing under the bridge. Previous field testing experience indicated problems with the electronic equipment were likely when

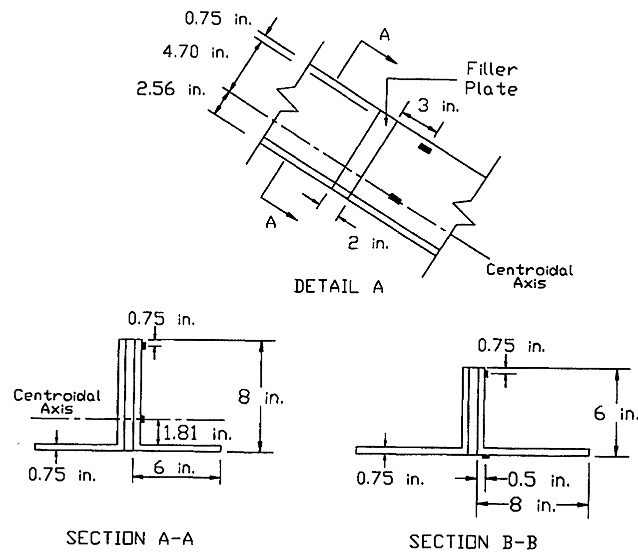

Fig. 5. Typical strain gage locations.

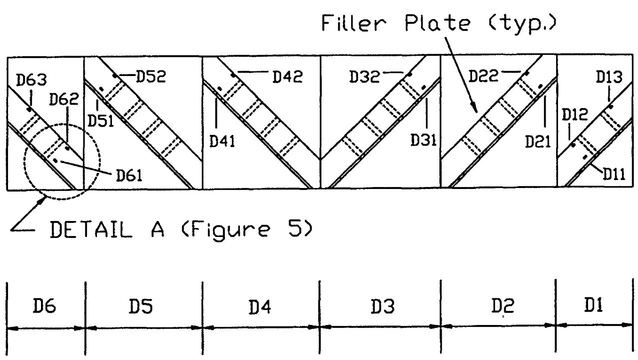

Fig. 4. Strain gage locations on diagonal members.

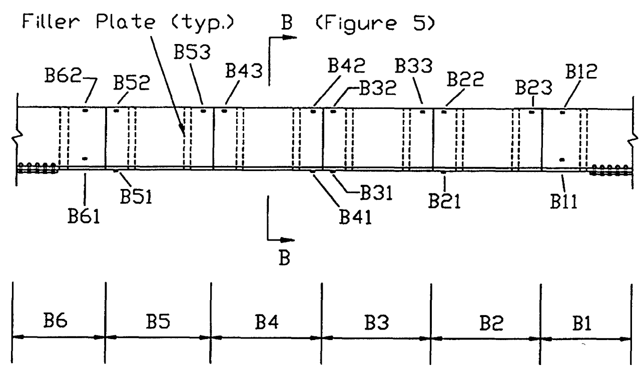

Fig. 6. Strain gage locations on bottom chord members.

recording data under hot and humid conditions. Therefore, an environmental chamber was used to protect the computer and data acquisition system from the heat and humidity common at the test sight. Shielded cables were used to connect all strain gages to the data acquisition system in order to minimize electronic noise in the data.

FIELD TEST RESULTS

The field test results indicate that the largest live load stress ranges near the filler plates occurred in the outside four diagonal members D1, D2, D5 and D6. Hence, the results regarding the potential for fatigue cracking in those members will be the focus of the discussion here.

Axial strain records for member D2 resulting from a 3-axle and a 5-axle test truck of known weight crossing the bridge at normal traffic speed are shown in Figure 7. These plots are representative of strain records for trucks in the normal traffic. The primary difference between the strain records is the single sharp peak for the short truck and the double peak for the long truck. The double peak results from the time difference between the front and rear tandem axles crossing the instrumented floortruss. The double peak did not appear in the strain records for all truss members for all long trucks

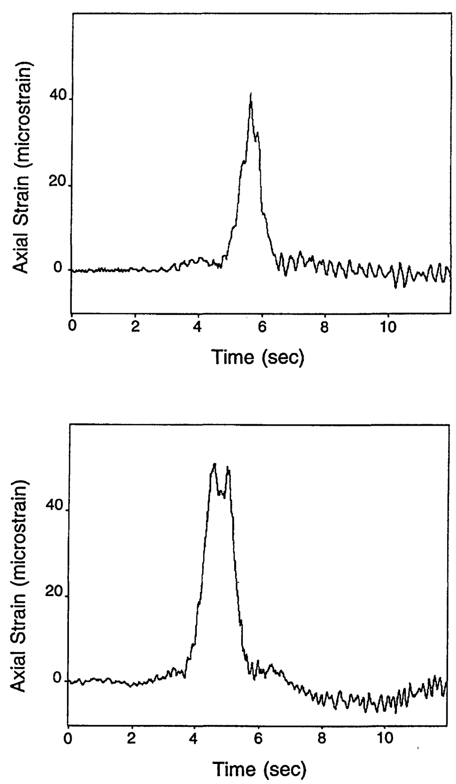

Fig. 7. Axial strain records for member D2 at quarter-span floortruss due to test truck crossings in the slow lane: (a) 3-axle truck; (b) 5-axle truck.

Table 1.
Stress Ranges (ksi) at Critical Extreme Fiber Locations

Stress Range	D1[a]	D2[b]	D5[b]	D6[a]
(A) Quarter-Span Floortruss				
5-axle, slow lane	2.2	2.2	1.9	1.7
5-axle, fast lane	1.7	2.0	1.8	2.1
Slow + fast lane	3.9	4.2	3.7	3.8
Traffic max.	4.2	4.4	4.0	3.9
Eff. stress range	2.1	2.2	2.0	1.7
(B) Mid-Span Floortruss				
5-axle, slow lane	1.9	1.8	1.2	1.7
5-axle, fast lane	1.5	1.9	1.1	1.9
Slow + fast lane	3.4	3.7	2.3	3.6
Traffic max.	4.2	4.4	3.0	3.4
Eff. stress range	1.9	1.8	1.2	1.6

[a]Stress ranges at top fibers at lower end of member.
[b]Stress ranges at bottom fibers at upper end of member.

crossing the bridge. Many of the strain records exhibited more of a plateau than a double peak while a long truck crossed the floortruss. Although the plots of Figure 7 indicate both positive and negative strain, the plots are for live load only, and the combined live load and dead load strain was always tensile. The gradual changes in strain that occur before and after the primary response due to the truck result from secondary effects of the truck crossing the 800 ft. tied arch span such as differential deflections between the tie girders.

To convert the strain records to stress ranges for use in the fatigue evaluation, each truck crossing was assumed to create one load cycle. The strains were converted to stress by multiplying by the modulus of elasticity of steel, 29,000 ksi. The magnitude of the stress range was taken as the difference between the maximum and minimum measured stresses. This approach neglects some fatigue damage accumulation due to secondary cycles such as the decrease in stress that occurs between the crossing of the front and rear tandem axles of typical 5-axle trucks. Neglecting the fatigue damage due to the secondary cycles is believed to cause no more error here than other common assumptions made in the fatigue analyses. For cases where the strain gages were not placed directly on the extreme fibers, stress ranges at the extreme fibers were determined by linear extrapolation of the stress ranges measured at the strain gage locations.

Stress ranges measured at critical extreme fiber locations (or linearly extrapolated to the extreme fibers) on the diagonal members are shown in Table 1. The stress ranges listed are for the extreme fiber location adjacent to a filler plate at which the maximum stress ranges occurred. Stress ranges produced by the passing of the 5-axle test truck in the slow and fast traffic lanes are listed in Table 1. The weight and axle configuration of the 5-axle truck was representative of the heavy trucks traveling the interstate carrying approximately the full

Table 2.
Percent Increase in Stress Ranges at Critical Extreme Fiber Locations Due to Bending

Member	Quarter-Span Floortruss	Mid-Span Floortruss
D1[a]	23	20
D2[b]	17	17
D5[b]	13	5
D6[a]	29	18

[a]Stress ranges at top fibers at lower end of member.
[b]Stress ranges at bottom fibers at upper end of member.

legal load. The gross weight of the 5-axle truck was 82.8 kips for the tests at quarter-span and 81.2 kips for the tests at mid-span. The sum of the stress ranges for the slow and fast lanes (labeled as "slow + fast lane" in Table 1) is also shown to provide an estimate of a worst case loading due to side-by-side heavy trucks. This sum can be compared to the "Traffic max." stress range measured from normal traffic. The "Traffic max." values are the largest stress ranges from 250 recorded events. The data acquisition system was configured so that a heavy loading that created an axial stress greater than 0.7 ksi in member D2 was recorded as a single event. Seven to eight hours was required at each floortruss location to record the 250 events.

The stress ranges in Table 1 illustrate that the maximum values recorded from normal traffic agree reasonably well at the mid-span and quarter-span floortrusses, especially for the most heavily loaded members D1 and D2. The agreement provides reasonable confidence that the "Traffic max." values are at the upper end of the normal traffic induced stress ranges since the data was taken on different days. The sum of the stress ranges for the slow and fast lanes tend to be smaller than the maximum value from normal traffic. The reason for this is unclear.

Effective stress ranges calculated using the 250 stress ranges from the normal traffic are also listed in Table 1. The effective stress ranges were calculated using the well known summation for the Miner's effective stress range (also called the root-mean-cubed effective stress range.) The largest effective stress ranges were found at members D1 and D2. Note that these effective stress ranges are very close to the values shown for the 5-axle test truck in the slow lane. This comparison provides confirmation that the 5-axle test truck was representative of most trucks crossing the bridge and that the slow lane was the most heavily travelled.

The relative magnitudes of the extreme fiber stress ranges due to bending and axial load are of interest for the fatigue analysis. Plots of maximum stress range (extreme fiber stress range) versus axial stress range were made from the normal traffic data as shown in Figure 8. Each point in Figure 8 represents the result of a single event from the normal traffic data. The slope of the best fit line through the data is the average ratio of extreme fiber stress to axial stress. Hence, for the data shown in Figure 8, the increase in stress range at the extreme fiber due to bending above the axial stress range is 23 percent. Similar plots were made for the other members, and Table 2 lists the percent increase in stress range at the extreme fiber due to bending for the critical extreme fiber locations referred to in Table 1. The increase varies from 5 to 29 percent for the critical locations of interest here. Study of the stress ranges in other members of the floortrusses revealed increases above the axial stress range due to bending of over 100 percent. However, the magnitudes of the stress ranges were significantly smaller than at the critical locations referred to in Table 1. The field test data also indicated that the increase in extreme fiber stress due to bending depended on the lane position of the truck causing the stress range (slow lane or fast lane) for diagonals D3 and D4. This dependence on lane position was not found for diagonals D1, D2, D5 and D6, so data from trucks in the slow and fast lanes plot along a single line as in Figure 8.

FATIGUE EVALUATION—COMPARISONS WITH DESIGN

Bridge designs are currently done in accordance with American Association of State Highway and Transportation Officials (AASHTO) specifications.[3] In the AASHTO procedure, the calculated nominal stress range in the base metal at a welded detail due to standard design truck loadings are compared to the fatigue strength of a category of similar details. Because an interstate highway bridge will eventually experience a very large number of load cycles, the calculated stress range is compared to the fatigue limit for the category.

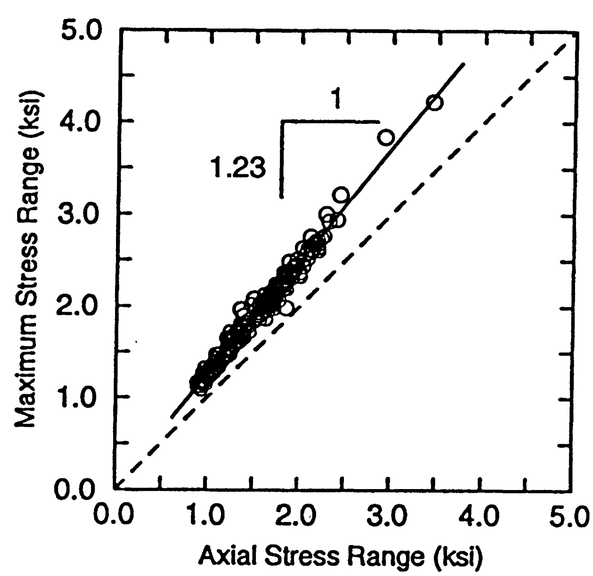

Fig. 8. Extreme fiber and axial stress ranges from normal truck traffic.

The most fatigue prone areas in the double angle tension members of interest here are at the welded connections to the gusset plates at the member ends and at the filler plate welds. The welds to the gusset plates at the member ends are the most severe detail (AASHTO Category E), and the fatigue limit at those details is 5 ksi. From the field tests, the maximum stress range recorded in any member was 4.4 ksi which is less than the fatigue limit of 5 ksi. Although the bending stresses at the member ends are somewhat higher than at the filler plate locations where the measurements were made, the field test results indicate that the actual stress conditions in the floor-truss members are not worse than assumed in the design process.

The fatigue limit at the filler plate welds before cracking due to pack rust is 10 ksi (AASHTO Category C). Visual inspection of the welds at a number of connections where cracking has not occurred did not reveal any deviations from normal steel fabrication practices which would reduce the fatigue limit for those details. Thus, fatigue cracking in the double angles at the filler plate welds as originally installed does not appear likely.

After the filler plate welds have cracked (failed) due to pack rust, the details do not clearly fall into an AASHTO fatigue category. A judgement about the conditions existing after a filler plate weld cracks suggests that failure of the weld does not significantly reduce the fatigue strength of the double angle. Specifically, the fatigue strength is not believed to be less than that of the Category E details at the ends of each member. When a filler plate weld cracks, the stress concentration effect of the change in cross section at the filler plate is eliminated. A new stress concentration is created by the rough surface of the broken weld. However, because the throat of the filler plate welds was initially very small, the roughened area is small and does not appear to have sufficient notch depths to create a significant stress concentration that is worse than the original uncracked condition. The effects of the surface roughness are also reduced somewhat by the normal weathering that occurs in a relatively short time after the welds break. Hence, there does not appear to be a significant risk of fatigue cracking in the double angles at locations where the filler plate welds have failed.

A limited number of the cracked filler plate welds have been repaired by field welding. In most cases the repair welds appear sound, and the repairs can be considered as a Category C detail. Thus, the repair welds do not pose a problem. However, slight undercut occurred at the ends of some of the repair welds. This condition is discussed further in the following sections.

FATIGUE EVALUATION—FRACTURE MECHANICS APPROACHES

The observations and judgements of the previous section suggest that fatigue cracking in the double angle tension members is not likely to occur. Additional insight regarding the performance of the double angle members can be gained from observations and estimations made using linear elastic fracture mechanics and fatigue crack growth calculations. The results of most interest are comparisons of the predicted behavior if a fatigue crack formed in the double angle member at the end of the filler plate weld for the following cases: (1) the original design, (2) at a cracked filler plate weld, and (3) at a welded repair of a cracked filler plate weld.

Based on the principles of linear elastic fracture mechanics, brittle fracture due to rapid crack extension occurs when the stress intensity factor, K_I, for a sharp tip crack reaches a critical value, K_c or K_{IC} (fracture toughness). The stress intensity factor is a mathematically calculated quantity that is a function of the plate geometry, crack geometry (length and shape), and the magnitude and distribution of stress acting on the plane of the crack. The crack length which results in brittle fracture for a given geometry and stress conditions is referred to as the critical crack length, a_{cr}.

Assumptions and Methods Used in Critical Crack Size and Fatigue Life Calculations

Material toughness tests were not performed for the double angle members. For the comparisons discussed below a toughness, K_c, of 50 ksi$\sqrt{\text{in.}}$ will be assumed. As discussed by Barsom and Rolfe,[4] the goal of quality control tests (Charpy V-Notch tests) required by AASHTO for bridge steels is to insure sufficient toughness that failures will not occur in a plain strain manner at the minimum expected service temperature and maximum load rate. A toughness of 50 ksi $\sqrt{\text{in.}}$ is not guaranteed by the tests. The assumed toughness is representative of bridge steels with yield strength of 50 ksi at a minimum service temperature of −30 degrees Fahrenheit and an intermediate strain rate of 10^{-3} sec^{-1}.

The types of fatigue cracks of particular interest here are cracks that may form at the extreme fibers of the back to back legs of the double angles at the end of the filler plate welds. The largest stress intensity values for a given crack length will occur at an edge crack of the type shown in Figure 9. A simplifying assumption is made that the edge crack will initiate and propagate with a straight crack front as shown in Figure 9. A fatigue crack at the opposite extreme fiber would initiate as a corner crack and would probably grow somewhat faster along the outstanding leg of the angle and eventually grow through the member as shown in Figure 9. For a given level of extreme fiber stress this process is assumed to require a larger number of load cycles for the crack to reach a critical length than for the edge crack to reach a critical length. Hence, the discussions below are limited to the edge crack geometry.

By considering combined dead load and live load effects the stress conditions at member D1 result in the smallest critical crack lengths, and the discussions below are based on the stress conditions at member D1. However, the fundamental conclusions drawn from the analyses apply to all the tension members and filler plate locations. Critical crack lengths were determined by calculating stress intensity factors which include the effects of the nonuniform stress distribution at the end of the filler plate welds. A stress distribution across the depth of the double angle members was developed by combining the linear distribution of stress due to bending and axial load with the stress concentration effect of the welded filler plate. The two separate stress distributions are shown in Figure 10. As determined from the field tests, live load bending stresses are created in the floortruss members by truck loadings. For the critical member D1 the level of bending was found to be independent of load position. Because the load position was not important, the same ratio of extreme fiber bending stress to axial stress was assumed to apply to the dead load stress created by the weight of the deck system. The axial dead load stress was determined to be 6.3 ksi from a structural analysis, and the field tests indicate that extreme fiber bending stress is 23 percent larger. As shown in Table 2 the largest measured extreme fiber live load stress range for member D1 was 4.2 ksi. Here the maximum live load stress due to traffic was also assumed to be 4.2 ksi. The measured value is the nominal extreme fiber stress which does not include the stress concentration effect of the filler plate. Fisher[5] et al. found for short attachments to beam flanges, that the stress concentration factor (SCF) is approximately 3. Here a stress concentration factor of 3 was used, and similar to assumptions by Fisher[5] et al. the stress concentration effect was assumed to diminish parabolicly to zero at a distance across the member equal to the filler plate length along the member (2 inches). The compression zone necessary for the stress distribution due to the stress concentration to be self-equilibrating was conservatively disregarded. As shown in Figure 10, a load factor of 1.3 was multiplied by the service load stresses for determination of the critical crack lengths. The load factor 1.3 is the value used in calculation of operating ratings (load capacities) for bridges according to the AASHTO Manual for Maintenance Inspection of Bridges.[6]

Critical crack lengths were determined for the three cases previously mentioned. The first case was for the original design. For that case, the stress concentration effect applies to both the dead load and live load. The second case was for an angle at a cracked filler plate weld. There is no stress concentration effect for this case, and only the linear distribution of nominal dead load and live load stress was used. In the third case, the stress concentration is relieved from the dead load when the original filler plate weld fails, but the stress concentration occurs for live loads after the crack is repaired by rewelding. For these three different stress distributions, stress intensity factors were calculated by integration using the Green's Function given by Broek[7] for edge cracks as shown in Figure 11. The numerical integrations required were carried out by breaking the crack length into 100 subdivisions. The results of the calculations are plotted in Figure 12.

Fatigue crack growth calculations were performed using the effective stress range shown in Table 2 for member D1. The tabulated stress range is the nominal extreme fiber stress range. For the original design and for the welded repair, the stress concentration effect as described above was used along with the linear variation of stress to account for bending. Only the linear variation to account for bending was used for the case of a cracked filler plate weld. The Green's Function approach described above was used to calculate stress intensity factor ranges. The crack growth calculations were per-

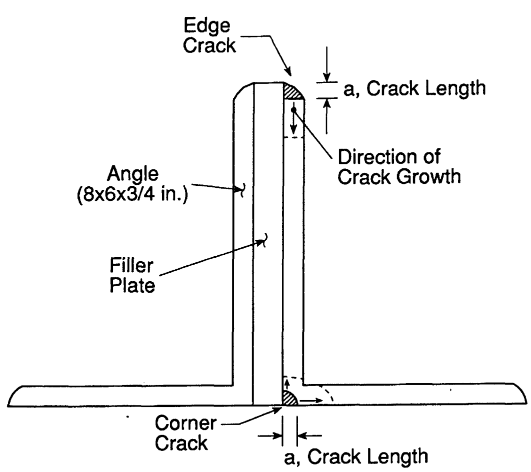

Fig. 9. Possible fatigue crack locations.

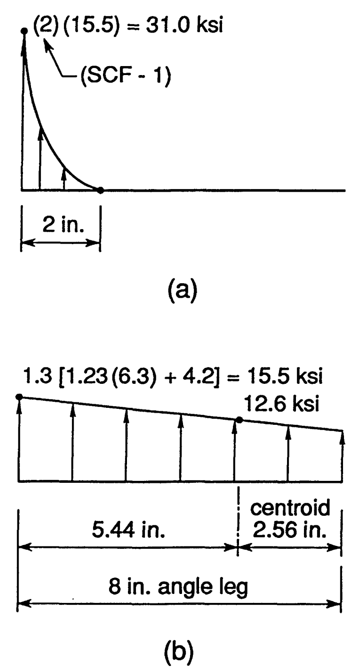

Fig. 10. Stress distributions near a filler plate.

formed using the following rate equation for ferrite-pearlite steels reported by Barsom and Rolfe[4]

$$\frac{da}{dN} = 3.6 \times 10^{-10} (\Delta K_I)^{3.0} \tag{1}$$

where

(da/dN) = the crack growth rate, and
ΔK_I = is the stress intensity factor range.

The calculations were carried out by numerical integration using a crack growth increment of 0.05 inches. The number of cycles, N, determined from the crack growth calculations were converted to a number of years at the current level of truck traffic (547,500 heavy vehicles per year) and are plotted in Figure 12.

Discussion of results

Stress intensity factors as a function of crack length are plotted in Figure 11 for an assumed crack for the three cases of interest mentioned above: (1) the original design, (2) a cracked filler plate weld, and (3) a welded repair of a filler plate weld. Also shown in Figure 11 is a plot of the stress intensity factor calculated for an edge crack in a zone of residual stress equal to the yield strength of the material (50 ksi) which may be present near the end of a filler plate weld.

For a critical stress intensity factor of 50 ksi$\sqrt{\text{in.}}$, the critical crack sizes from Figure 11 are seen to be 1.99 inches for the welded repair and larger than 2.5 inches (3.02 inches) for the case of a cracked filler plate weld. These are quit large compared to 0.41 inches for the original condition. The differences result from the changes in the stress concentration at the filler plate. Because there is no stress concentration at the cracked filler plate weld, that case has the longest critical crack length. At the welded repair, the critical crack length is somewhat shorter because there is a stress concentration for the live load stress. The stress concentration applies to both live load and dead load for the original condition which results in the shortest critical crack length. Because the material toughness was assumed each of these estimated critical crack lengths may be shorter than for the actual conditions, but they provide realistic comparisons.

The stress intensity factor plot for the assumed residual stress provides a means for an approximate evaluation as discussed by Barsom and Rolfe[4] of the effects of residual stresses near the welds in the original design and for the repair weld. It is not uncommon for residual stresses at or near the yield strength of the material to form in the base metal around a weld due to shrinkage as the weld cools. Residual tension results near the weld and residual compression a short distance away. If the material toughness is very low, fracture could result for very short cracks confined to the zone of residual stress. With sufficient material toughness, as a crack forms and propagates through the zone of residual stress, the residual stress is relieved. For the particular welds of interest here which are approximately 0.25 inches or less, it is likely that the zone of high residual stress in 0.5 inches or less in diameter. From Figure 12, it is seen that the stress intensity factor for the residual stress equal to the yield stress reaches the critical value of 50 ksi$\sqrt{\text{in.}}$ at a length of 0.32 inches Before a crack could reach a length of 0.32 inches from fatigue propagation, it is likely that the residual stress would be significantly reduced so that fracture would not result. Hence, the zone of residual stress near the welds at the original condition and at the repair welds are assumed not to control the critical crack length.

Plots of fatigue lives for the three cases of interest are shown in Figure 13. Because the live load stress range and stress concentrations for the original and repair weld condi-

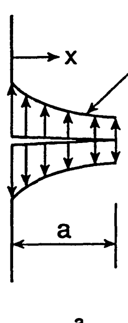

$\frac{x}{a}$	C
<0.6	1
0.6-0.7	1.01
0.7-0.8	1.03
0.8-0.9	1.07
>0.9	1.11

$$K_I = \int_0^a \sigma \, G \, dx$$

$$G = \frac{2C}{\sqrt{\pi a}} \; \frac{[-0.4(x/a)^2 + 1.3]}{\sqrt{1-(x/a)^2}}$$

Fig. 11. Green's function for an edge crack from Broek.[7]

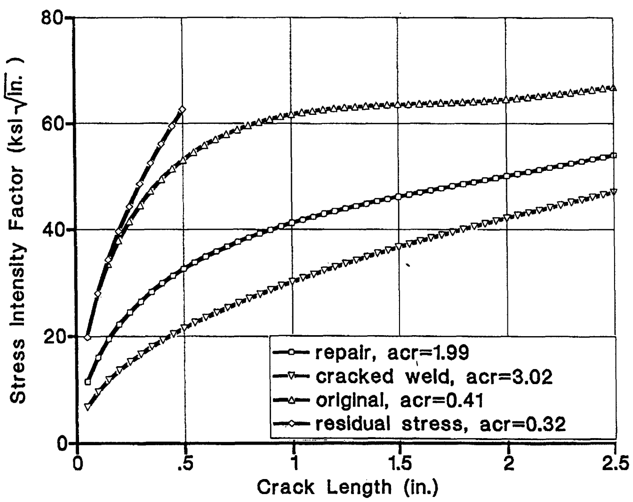

Fig. 12. Stress intensity factors due to factored dead load plus live load.

tions are the same, the same fatigue life plot applies to both cases, but the critical crack lengths are different as shown. Each of the fatigue life plots are assumed to start at an initial crack size of 0.225 inches This is somewhat of an arbitrary choice, but it provides a reasonably visible (detectable by visual inspection) crack size which is sufficiently long so that the residual stresses near the welds would be reduced significantly. The times required to reach a crack of 0.225 inches are ignored for purposes of this discussion although the times may be very long and will not be equal for the three cases.

The fatigue performance for the cases of the repair weld and the cracked filler plate weld are superior to the original condition as shown in Figure 13. Just over 4 years is required for a crack at one of the original connections to reach the critical crack size while approximately 19 years is required at a repair weld. Fatigue crack growth at a cracked filler plate weld is seen to be very slow. Visual inspections of bridges are performed at intervals not exceeding 2 years. Hence, at one of the original welds the results in Figure 13 indicate that a fatigue crack would have to be overlooked in two consecutive inspections before it could reach a critical length. At a repair weld, a fatigue crack would have to be overlooked 9 times, and 4 of these would be after the crack reached a substantial length in excess of 1 in. Crack growth at a cracked filler plate weld would be so slow that it is practically impossible for a crack to reach a critical length without detection.

The above results indicate that the performance after a filler plate weld cracks (fails due to pack rust) is superior to the original condition whether or not the cracked weld is repaired or left unrepaired. Based on the fatigue analyses, the best performance results from no repair which, fortunately, requires no maintenance expenditures. These basic conclusions would also be reached even if better estimates of the material toughness were available and if an elastic-plastic fracture methodology was used for the analysis. The conclusion is also not sensitive to the precise magnitude of the stress concentration at the filler plate since the differences in performance result from whether or not there is a stress concentration

SUMMARY AND CONCLUSIONS

Based on field test data, the four outer diagonals (D1, D2, D5, and D6) were found to be the most highly stressed members in the floortrusses. For these four members, the nominal extreme fiber stress ranges near the filler plates due to axial load plus bending varied from 5 to 29 percent higher than the axial stress ranges. The percentage increases in stresses due to bending in these members was found to be unaffected by truck weight or lane position.

The highest nominal stress range near a filler plate found through field testing was 4.4 ksi, and stress ranges of this magnitude occurred at the upper end of member D2 at both the mid-span and quarter-span test locations. These worst case values are less than half the AASHTO fatigue limit of 10 ksi for the original filler plate weld details and are not large enough to cause fatigue cracks to develop in the double angle members. Fatigue cracking is not expected to occur in the double angle members after the filler plate welds fail due to pack rust because the failure surfaces are relatively smooth. The failure surfaces are relatively smooth due to the small original weld size and the weathering of the A588 steel.

Predictions of the fatigue life of the double angle tension members based on fracture mechanics principles indicate that the possibility of fatigue cracking at cracked filler plate welds does not pose an unusually great threat to the integrity of the tied arch span floortrusses. The fatigue life was found to be improved after a filler plate weld fails because the stress concentration due to the filler plate is removed. Fatigue life calculations also indicate that if fatigue cracks initiate in the double angles, the cracks will grow at a sufficiently slow rate to be found in the normal two year bridge inspections.

ACKNOWLEDGEMENTS

Financial support for this project was provided by the Alabama Department of Transportation and the Auburn University Highway Research Center. Valuable assistance during the field tests was provided by Scott K. Rutland and numerous personnel from the Maintenance Bureau and Ninth Division of the Alabama Department of Transportation. For all this, the authors are grateful.

REFERENCES

1. Kulicki, J. M., Prucz, Z., Sorgenfrie, D. F., Mertz, D. R. and Young, W. T., "Guidelines for Evaluating Corrosion Effects in Existing Steel Bridges," National Research Council, *Transportation Research Record 333*, Washington, D.C., 1990.

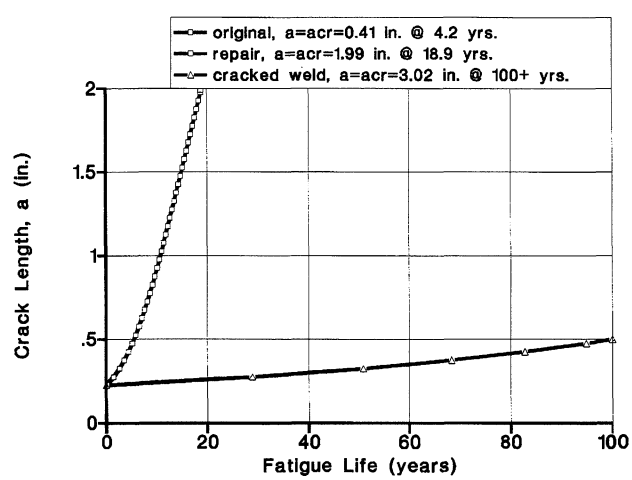

Fig. 13. Fatigue lives of double angle tension members.

2. Stallings, J. M., Cousins, T. E. and Christopher, B. P., "Evaluation of Fatigue Cracking in Mobile Delta Crossing Bridges, Volume II Filler Plate Weld Cracks," Highway Research Center, *Project No. ST-2019-16*, Auburn University, Auburn, AL, 1993.
3. American Association of State Highway and Transportation Officials, *Standard Specifications for Highway Bridges*, 15th Ed., Washington, D.C., 1993.
4. Barson, J. M. and Rolfe, S. T., *Fracture and Fatigue Control in Structures*, 2nd Ed., Prentice-Hall, Englewood Cliffs, NJ, 1987.
5. Fisher, J. W., Albrecht, P. A., Yen, B. T., Klingerman, D. J. and McNamee, B. M., "Fatigue Strength of Steel Beams with Welded Stiffeners and Attachments," National Research Council, *NCHRP Report 147*, Washington, D.C., 1974.
6. American Association of State Highway and Transportation Officials, *Manual for Maintenance Inspection of Bridges*, Washington, D.C., 1983.
7. Broek, David, *The Practical Use of Fracture Mechanics*, Kluwer Academic Publishers, Boston, MA, 1989.